

1 Epitaxial refractory-metal buffer layers with a chemical gradient for 2 adjustable lattice parameter and controlled chemical interface

3 O. Fruchart,^{1, a)} A. Rousseau,¹ D. Schmaus,^{2,3} A. L'Hoir,^{2,3} R. Haettel,¹ and L. Ortega¹

4 ¹⁾*Institut Néel (CNRS and Université Joseph Fourier), BP166, F-38042 Grenoble Cedex 9,*
5 *France*

6 ²⁾*Institut des NanoSciences de Paris (INSP) (CNRS UMR 7588 and UPMC Université Paris 6), 4 place Jussieu,*
7 *75252 PARIS Cedex 05, France*

8 ³⁾*Université Paris Diderot-Paris 7, 75205 Paris Cedex 13, France*

9 (Dated: 18 October 2018)

10 We have developed and characterized the structure and composition of nanometers-thick solid-solution epi-
11 taxial layers of (V,Nb) on sapphire (11 $\bar{2}$ 0), displaying a continuous lateral gradient of composition from one to
12 another pure element. Further covered with an ultrathin pseudomorphic layer of W, these provide a template
13 for the fast combinatorial investigation of any growth or physical property depending of strain.

14 Thin films play a crucial role in integrated technology, 53
15 and it is necessary to control their physical properties. 54
16 In a down-scaling approach one seeks to sustain the bulk 55
17 properties. One may also endeavor to tailor new proper- 56
18 ties that do not occur in the bulk, an approach being one 57
19 basis for the development of nanosciences. The parame- 58
20 ter often at play in the change of properties in thin films is 59
21 strain¹, influencing *e.g.* mobility in semiconductors², op- 60
22 tical activity, electric polarization or magnetic moment³ 61
23 and anisotropy⁴. The easiest way to control strain in thin 62
24 film is through their epitaxy on substrates with a lattice 63
25 parameter different from their own, inducing a so-called 64
26 lattice misfit. Lattice misfit also influences growth modes 65
27 (smooth or rough films, islands...) ^{5,6}, which strengthens 66
28 the need for its control. 67

29 Effects of lattice misfit are often investigated by growth
30 on single crystals of various pure elements, each with
31 a well-defined lattice parameter. Alloys and solid solu-
32 tions (s.s.) are an appealing combinatorial alternative
33 as they allow for the continuous control of lattice misfit,
34 which is not possible for pure elements⁷. Nevertheless,
35 systematic studies with s.s. require several samples with
36 different compositions, with issues of time, reproducibil-
37 ity and limited number of data points. To circumvent this
38 Kennedy *et al.*⁸ have introduced compositional spreads,
39 where the anisotropy of evaporation of two sources are
40 used to create a slight gradient of composition across
41 a sample. Later, alternated deposition of the materials
42 along with moving masks were used to create intercalated
43 wedges of two or three elements^{9,10}. This allows one to
44 vary the composition linearly and potentially from 0%
45 up to 100%. In these seminal uses of masks the alloy
46 resulted from a post-annealing, which is not suited for
47 most epitaxial and thin films. Only Zhong *et al.* applied
48 this technique to epitaxial materials (semiconductors),
49 however restricted it to the case of weak doping¹¹.

50 We issued a preliminary report of chemical gradients
51 with controlled chemical surface¹², however with a neg-
52 ligible variation of lattice parameter via mixing body-

centered cubic (bcc) Mo (lattice parameter 3.157 Å) and
W (3.165 Å), therefore with virtually no metallurgical is-
sues and with restricted practical use. Here we report
the fabrication, the structural, composition and surface
characterization of epitaxial Chemical-Gradient Layers
(CGLs) of bcc refractory metals, in the full range of com-
position to adjust the lattice parameter over 10%. Fur-
ther combined with an ultrathin pseudomorphic layer,
these provide a versatile buffer-layer toolkit for the elu-
cidation and use of the many phenomena depending on
lattice mismatch.

The samples were grown using Pulsed-Laser Deposi-
tion in a set of Ultra-High-Vacuum chambers. The laser
is a 10 Hz-pulsed Nd-YAG laser with pulse length \approx 10 ns
and doubled frequency ($\lambda = 532$ nm). The deposition
chamber is equipped with a computer-controlled mask
moving in front of the sample, and 10 kV Reflection High
Energy Electron Diffraction (RHEED)¹². Our CGLs are
based on mixtures of two bcc elements (Mo, W, Nb, V),
that all form s.s. one with another. Results are illus-
trated in this Letter with the case of (V,Nb). (11 $\bar{2}$ 0) sap-
phire wafers are used as a support, resulting in the (110)
texture of the films^{12,13}. Searching for an optimized pro-
cedure, CGLs were grown directly on 0.7 nm-thick-Mo-
dusted sapphire wafer (Mo is inserted to avoid crystallo-
graphic variants¹²), or on an atomically-flat 10 nm-thick
W(110) buffer layer itself above Mo-dusted sapphire. The
wedges of the two elements are deposited sequentially,
in an opposite fashion thanks to the azimuthal rota-
tion of the sample of 180°. The length of the wedges
is 5 mm (FIG. 1a). Their typical thickness is 1 Å, which
is less than one atomic layer, with a view to promote
the mixture of both elements at the atomic level and
avoid the formation of misfit dislocations that would oc-
cur for thick individual layers. Deposition is performed
at moderate temperature (300 °C), followed by anneal-
ing for 30 min at 800 °C to smoothen the surface. The
typical total thickness of these films is 10 nm.

FIG. 1 shows RHEED patterns and Scanning Tunnel-
ing Microscopy (STM) images of a (V,Nb)/Mo(0.7 nm)
CGL directly grown on sapphire. The RHEED streak
narrowness, large terrace size and absence of emerging

^{a)}Olivier.Fruchart@grenoble.cnrs.fr

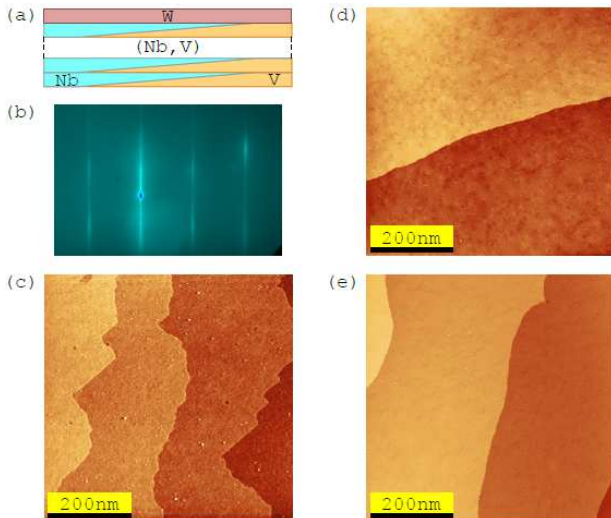


FIG. 1. (a) Schematics of a CGL, further covered by an ultrathin W layer for the chemical control of the free surface. (b) typical RHEED pattern, for electron azimuth $[1\bar{1}0]$ (the bright spot is the reflected beam). STM images of (V,Nb)/Mo(0.7 nm)/Al₂O₃ CGLs (not covered with an ultrathin W layer) for (c) V, (d) V₅₀Nb₅₀ and (e) Nb .

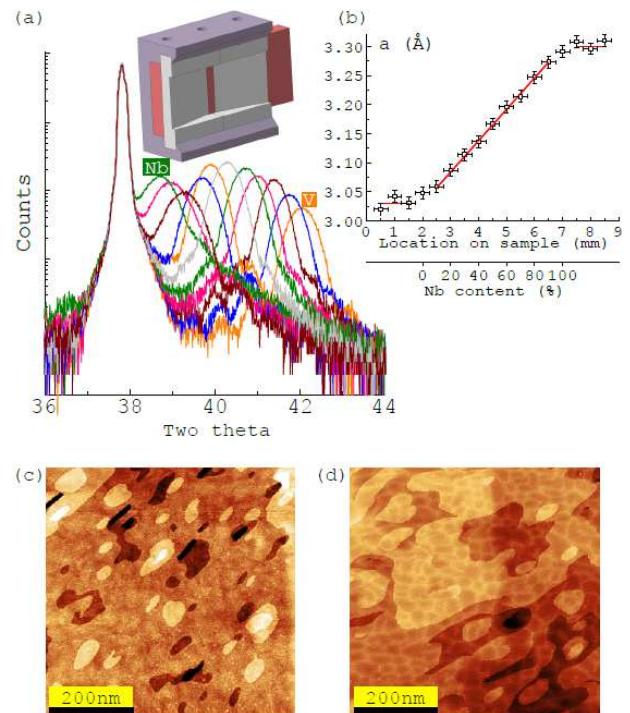


FIG. 2. (a) $\theta-2\theta$ diffraction spectra of (V,Nb)/Mo(0.7 nm)/Al₂O₃ CGLs. At 37.85° is a sapphire peak. Inset: mask used to select the area of interest for diffraction (b) Extracted from (a), out-of-plane lattice parameter as a function of composition along the CGL. Lines are the expectation of Vegard's law. STM images of ultrathin layers of W of thickness (c) 0.6 nm and (d) 2 nm on a CGL.

1 screw dislocations, provide a picture of a high-quality
2 crystal. No significant difference is found in RHEED and
3 STM data as a function of the local composition, from
4 pure V to pure Nb, with or without an underlying W
5 buffer layer.

6 We developed a sample holder to perform X-Ray
7 Diffraction over a small and precise location on the
8 sample. It consists of a 1 mm-wide window between
9 two steel blades machined at an angle of 12° to let
10 in and out X-rays down to grazing incidence. The
11 blades are covered with a $10\ \mu\text{m}$ -thick layer of metallic
12 glass ($\text{Zr}_{52.5}\text{Ti}_{2.5}\text{Cu}_{22}\text{Ni}_{13}\text{Al}_{10}$) to avoid diffraction from
13 the mask. A manual sample translator allows one to se-
14 lect the area of investigation (inset of FIG. 2a). FIG. 2a
15 shows $\theta-2\theta$ spectra as a function of location on the sam-
16 ple, translated into the expected composition. The oc-
17 currence of Kiessig fringes arises from the finite thickness
18 of the films and the absence of roughness. Their width
19 is composition-independent and consistent with the film
20 thickness. The films are thus coherent across their entire
21 thickness, showing their good layered structure, consis-
22 tent with STM data (FIG. 1c-e). The out-of-plane lat-
23 tice parameters extracted from these curves are shown
24 in FIG. 2b. The error bars result from the precision of
25 the lateral position of the sample, and from the com-
26 bined fitting of peaks and calibration of the diffractome-
27 ter against the first and second order peaks of sapphire.
28 Within the error bar the lattice parameter varies linearly
29 with composition and ranges from the bulk lattice pa-
30 rameter of V ($3.02\ \text{\AA}$) to that of Nb ($3.30\ \text{\AA}$), in agree-
31 ment with Vegard's Law. *in situ* RHEED yields the in-
32 plane lattice parameter, albeit with larger error bars (not

shown here). These also fit Vegard's law, demonstrat-
ing the good structural relaxation of the s.s.. Finally,
the CGLs may be covered by an ultrathin W layer de-
posited at 250°C and then annealed at 800°C , a pro-
cedure known not to give rise to intermixing with the
underlying film¹². STM shows that W remains pseudo-
morphous up to $\approx 1\ \text{nm}$ (FIG. 2c), above which relaxa-
tion is revealed by an array of misfit dislocations (FIG. 2d)¹⁴.
CGLs covered with this ultrathin pseudomorphic W layer
provide a surface with a continuously-variable lattice pa-
rameter, however with a uniform and a rather inert sur-
face material.

In order to check locally both the composition of the
s.s., and their crystalline quality, the samples were also
analyzed using Rutherford Backscattering Spectrometry
(RBS) both in random and channeling geometries (for
these analytical techniques, see Ref.¹⁵). Indeed, whereas
X-ray and electron diffraction probe long-range crys-
talline coherence and are mostly insensitive to local dis-
order, RBS in a channeling geometry is highly sensitive to
such disorder and is thus very valuable to refine the close-
to-perfect picture of CGLs given by FIG. 1 and 2. RBS
was performed within the SAFIR facility of the INSP,
using a $1.4\ \text{MeV}\ ^4\text{He}^+$ ion beam with a $0.5\ \text{mm}$ diameter,
produced by a $2.5\ \text{MV}$ Van de Graaff accelerator. The

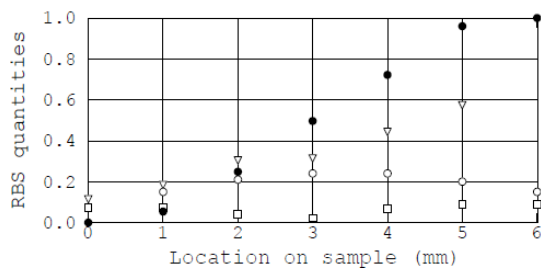


FIG. 3. Local quantities determined by RBS (random or channeling conditions), as a function of the location x across a (V,Nb)/W(10 nm)/Mo(0.7 nm)/Al₂O₃ CGL: Nb concentration (●), normalized channeling ([110] alignment) yields Y_{Nb} (○), Y_V (▽) and Y_W (□) (see text). The zero for the lateral scale is different from that of FIG. 2b.

ions scattered elastically at large angle (here $\approx 150^\circ$) on the sample nuclei (rare scattering events) were energy-analyzed using a silicon detector.

Conversely, the most probable scattering events result in small-angle repulsive deflections. When the incident beam is aligned with a major crystallographic axis of a crystal (channeling geometry, here performed along [110]), these deflections are correlated and the particle flux close to the rows is strongly reduced, leading to a similar reduction of the RBS yield Y with respect to the yield R using a random orientation of the beam. For convenience, in the following Y values are normalized to the corresponding RBS random yield. Whereas R_i values for element i are proportional to the absolute amount of i atoms in the layer, Y_i values are mostly sensitive to atomic displacements in the plane perpendicular to the channeling axis¹⁶.

Various samples were analyzed, but we only present here the case of (V,Nb) deposited on a 10 nm-thick W(110) buffer layer (FIG. 3). Both $R_V(x)$ and $R_{Nb}(x)$ exhibit a linear variation across the sample, their sum keeping a nearly constant value corresponding to a thickness of about 10 nm of the (Nb,V) layer. This provides a direct quantitative confirmation of the linear variation of composition [*e.g.* $C_{Nb} = R_{Nb}/(R_{Nb} + R_V)$] with x , suggested indirectly previously through the agreement with Vegard's Law (FIG. 2).

Concerning the crystalline quality of the s.s., the relatively high channeling yields Y_{Nb} and Y_V observed on FIG. 3, with a marked dependence on C_{Nb} , may hint at atomic displacements in the s.s., relatively far from the CGL-W interface (see below). Their precise identification needs further analysis. Despite this, paradoxically, the very low channeling yield Y_W in the range [0.02–0.05] is indicative of a very good epitaxy. The highest quality ($Y_W \approx 0.02$) is obtained for Nb_{0.5}V_{0.5}, for which there is no lattice mismatch between the alloy and W, in agreement with FIG. 2b.

To conclude, we developed high-quality epitaxial solid-

solution layers of refractory metals along the orientation (110), in the form of Chemical-Gradient Layers (CGLs). These CGLs were then covered with a flat and ultra-thin pseudomorphic layer of W(110). This combination provides a template with a lattice parameter varying laterally over 10 % and with a controlled and rather inert W chemical interface, which may be used for the fast combinatorial investigation of any growth or physical phenomenon depending on strain. This may be performed with local probes such as electron, optical or scanning-probe microscopies, or with many nowadays synchrotrons offering beams focused to 100 μ m or smaller.

ACKNOWLEDGMENTS

We acknowledge the contribution of J. L. Soubeyrou (CRETA, Grenoble) for providing bulk metallic glass for preliminary XRD slits, N. Dempsey (Institut Néel) for the deposition of thick films of metallic glass, V. Guisset and Ph. David for technical support with UHV and E. Briand for efficient help in RBS experiments. This work received financial support from FP6 EU-NSF program (STRP 016447 MagDot) and French National Research Agency (ANR-05-NANO-073 Vernanomag).

REFERENCES

- ¹R. E. Newnham, *Properties of materials - Anisotropy, symmetry, structure* (Oxford University Press, Oxford, 2005).
- ²M. V. Fischetti and S. E. Laux, *J. Appl. Phys.* **80**, 2234 (1996).
- ³V. L. Moruzzi, P. M. Marcus, and J. Kübler, *Phys. Rev. B* **39**, 6957 (1989).
- ⁴J. Buschbeck, I. Opahle, M. Richter, U. K. Rößler, P. Klaer, M. Kallmayer, H. J. Elmers, G. Jakob, L. Schultz, and S. Fähler, *Phys. Rev. Lett.* **103**, 216101 (2009).
- ⁵E. Bauer and J. H. Van der Merwe, *Phys. Rev.* **B33**, 3657 (1986).
- ⁶J. H. van den Merwe, *Phil. Mag. A* **45**, 159 (1982).
- ⁷P. Y. Friot, P. Turban, S. Andrieu, M. Piecuch, E. Snoeck, A. Traverse, E. Foy, and C. Theodorescu, *Europhys. J. D* **15**, 41 (2000).
- ⁸K. Kennedy, T. Stefansky, G. Davy, C. F. Zackay, and E. R. Parker, *J. Appl. Phys.* **36**, 2808 (1965).
- ⁹F. Tsui and L. He, *Rev. Sci. Instr.* **76**, 062206 (2005).
- ¹⁰V. Matias and B. J. Gibbons, *Rev. Sci. Instr.* **78**, 072206 (2007).
- ¹¹Y. Zhong, Y. S. Chu, B. A. Collins, and F. Tsui, *Appl. Surf. Sci.* **254**, 714 (2007).
- ¹²O. Fruchart, P. O. Jubert, M. Eleoui, F. Cheynis, B. Borca, P. David, V. Santonacci, A. Liénard, M. Hasegawa, and C. Meyer, *J. Phys.: Condens. Matter* **19**, 053001 (2007).
- ¹³G. Oya, M. Koishi, and Y. Sawada, *J. Appl. Phys.* **60**, 1440 (1986).
- ¹⁴H. Bethge, D. Heuer, C. Jensen, K. Reshöft, and U. Köhler, *Surf. Sci.* **331-333**, 878 (1995).
- ¹⁵D. Schmaus and I. C. Vickridge, "Analytical methods for corrosion science and engineering," (CRC, Taylor & Francis group, Boca Raton, 2006) p. 103.
- ¹⁶A detailed discussion of RBS-channeling data will be addressed separately.